Multi-Modal Superparamagnetic Nanoprobe: Harnessing Magnetic, Nuclear, and Optical Power for Diagnostic Imaging Applications

A. Bumb*, C.A.S. Regino*, M. Bernardo*, P.J. Dobson**, P. Choyke*, and M.W. Brechbiel*

*National Cancer Institute, Bethesda, MD, USA, bumba@mail.nih.gov, reginoc@mail.nih.gov, bernardom@mail.nih.gov, pchoyke@mail.nih.gov, martinwb@mail.nih.gov
**University of Oxford, Oxfordshire, UK, peter.dobson@eng.ox.ac.uk

ABSTRACT

Targeted, controlled, and noninvasive delivery of therapeutics is a major goal of pharmaceutical development. However, few techniques allow imaging and controlled drug release at the cellular level. Herein, a potential targeted drug delivery platform with three imaging reporters has been developed by coupling the magnetic properties of ultrasmall superparamagnetic iron oxide nanoparticles (USPIOs) with near infrared fluorescence of Cy5.5 and γ-emissions of ^{111}In that is chelated to a conjugated antibody. This silica-coated iron oxide nanoparticle (SCION) allows for verification of localization, characterization of nearby physiology, and quantification.

Keywords: cancer diagnostics, nanoparticle, magnetic resonance imaging, optical imaging, nuclear imaging

1 INTRODUCTION

Nanoparticle technology has attracted immense interest in the past two decades as a platform for non-invasive bioimaging; however, effective application relies greatly on robust nanoparticle engineering and synthesis techniques. While particle development involves design, synthesis, and surface modification, the performance of a nanoprobe relies on particle composition, size, surface charge, surface functionality, biocompatibility, contrast sensitivity, and stability [4].

Ultrasmall superparamagnetic iron oxide nanoparticles (USPIOs) have been proving to be a class of agents useful for *in vitro* and *in vivo* cellular and molecular imaging. Maghemite/magnetite, γ-Fe_2O_3/Fe_3O_4, particles have face-centered cubic packing of oxygen that allows electrons to jump between iron ions occupying interstitial tetrahedral and octahedral sites. This gives the agent half-metallic properties that shorten transverse relaxation times, T_2 and T_2*, and increase proton relaxivities ten-fold [4]. USPIOs, typically 5-12 nm, exhibit prolonged blood half-life that affords them the opportunity to have more widespread tissue distribution and delivery to the interstitium through non-specific vesicular transport and transendothelial channels. Once in the interstitium, draining lymphatic vessels transport them to lymph nodes, allowing them to be suitable agents for MR lymphography (MRL). Furthermore, iron-based nanoparticles have a well recognized metabolic fate *in vivo* that has been accepted by regulatory agencies.

The purpose of designing molecular imaging probes is to make particles that are targetable and imageable. Multimodal particles provide advantages that traditional single modality agents lack. While magnetic resonance imaging (MRI) is a non-invasive technique that has exquisite resolution, its sensitivity is lower than radioactive and optical methods. Optical imaging has the advantage of high spatial and temporal resolution but with limited depth penetration due to light diffusion through tissue. Imaging of radioisotopes using single photon emission computed tomography (SPECT) allows for quantification but with low spatial and temporal resolution. Combining the three imaging techniques could provide a most effective diagnostic tool. An USPIO that is labeled by both a radioisotope and optical contrast agent would permit high resolution imaging and quantification with the ability to verify that the particle has reached its target through three imaging modalities. Furthermore, for *in vitro* studies, fluorescent nanoparticles provide convenience with typical analysis tools such as confocal microscopy and flow cytometry, whereas the magnetic properties would allow for ease of separation by use of a strong magnet in techniques such as magnetic activated cell sorting (MACS). Particularly if it is removable, having the third imaging agent, the radioisotope, could provide great advantages for *in vivo* studies for quantification of delivered construct through biodistribution studies. Targeting these particles with biomolecules such as antibodies would create a noninvasive reporting tool used to monitor biological responses and provide valuable information regarding physiology and pathophysiology.

2 PARTICLE SYNTHESIS

In Bumb *et al* [2-3], we describe the synthesis and characterization of a dual-modality nanoparticle that combines the magnetic properties of USPIOs with the

fluorescence properties of the near infrared (NIR) fluorophore Cy5.5, a cyanine dye with excitation and emission peaks at 675/694 nm, superior photostability, and a high extinction coefficient (ε = 190000 $M^{-1}cm^{-1}$ in PBS) [15]. In the NIR region (~700 to 900 nm), the absorption coefficient of tissue is considerably smaller so light can penetrate more deeply into tissue to depths of several centimeters albeit with considerable diffusion [5, 22]. Additionally, NIR dyes minimize signal contamination from autofluorescence arising from intrinsic biomolecules typically occuring in the visible light spectrum, 350-700 nm [1, 21]. Cy5.5 is a standard dye used for NIR imaging, however the chemistry used for synthesis of the particle is interchangeable with other dyes amenable to this same conjugation chemistry. Because the dye is encapsulated within the silica, particle properties are expected to remain similar.

It is necessary to functionalize USPIOs with a surface coating, such as silica, that enhances stability and biocompatibility. Silica maintains stability for particle suspensions during changes in pH or electrolyte concentration due to silanol groups that make the surface lyophilic [16]. It is well known for optical transparency [10] and may also enhance photostability by providing a protective layer around encapsulated optical agents [17-18]. Specifically in this particle's case, Cy5.5 is highly lipophilic, which often contributes to its uptake and metabolism in the liver. The dye's encapsulation could improve biodistribution and prevent its release from the particle, while improving the stability of the dye itself. Silica is soluble in aqueous and non-aqueous solutions, resistant to swelling, non-toxic, resistant to microbial attack, and biocompatible [24, 8]. Particurly important to nanoprobe development, silica deposition can be controlled for a tunable layer thickness, and its silanol groups easily react with alcohols and silane coupling agents [19] for strong covalent bonding with ligands, such as proteins, peptides, sugars, antibodies and oligonucleotides.

To conjugate antibody (Ab) to the surface of the silica-coated iron oxide nanoparticles (SCION), the particles were maleimide-functionalized with a conjugate of APTES and sulfosuccinimidyl-4-(*N*-maleimidomethyl)cyclohexane-1-carboxylate (s-SMCC). The Abs were activated by conjugation to Traut's reagent [23] (~1.8 thiols per antibody), and the particle maleimides then formed strong covalent bonds with the antibody thiols. A number of antibodies have successfully been conjugated to the particles including L243, trastuzamab (Herceptin), and cetuximab (Erbitux). L243 is an anti–HLA-DR monoclonal antibody (mAb) that could be used to direct the particles to cells from the inflammatory foci in the brain of multiple sclerosis patients [9, 11]. Herceptin and Erbitux respectively target membrane bound receptors HER2 and HER1that are over-expressed in a variety of epithelial cancers, including breast, ovarian, pancreatic, and colorectal

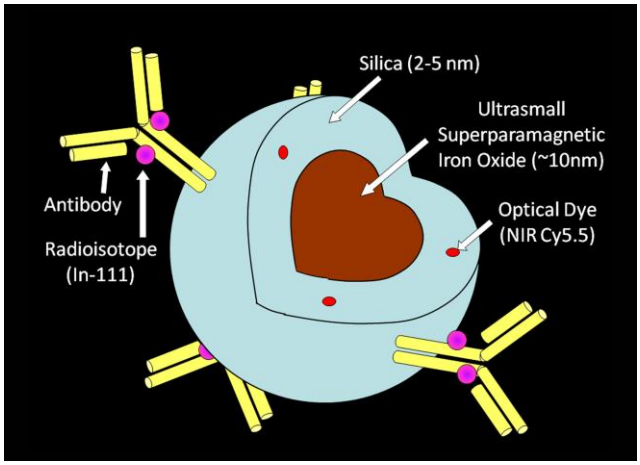

Figure 1: Tri-imageable nanoparticle

carcinomas [6, 13]. The chemistry used for ligand conjugation can be applied to other proteins and biomolecules as well.

The third imaging modality was attached using the chelate 2-(p-isothiocyanatobenzyl)-cyclohexyl-diethyl enetriaminepentaacetic acid (CHX-DTPA). Chelate isomer CHXA"-DTPA provides efficient labeling with ^{111}In and demonstrates maintenance of integrity and immunoreactivity of its radioimmunoconjugates [7, 12]. In the case of particles that were being radiolabeled, the chelate was attached to the antibody before thiol-activating it with Traut's reagent. The chelation chemistry is described by [14], where on average 1.9 chelates were attached per antibody. High yields of 77% have been achieved during radiolabeling of chelated Ab-SCION with Indium-111.

The final structure of the developed particle is shown in Figure 1.

3 PARTICLE CHARACTERIZATION [2-3]

A number of SCION properties were characterized and are summarized in Table 1. Size was analyzed by transmission electron microscopy (TEM) and dynamic light scattering (DLS). For TEM, multiple samples were drop-cast onto carbon grids, images collected with a JEOL4000EX microscope, and Gatan Digital Micrograph 3.6.1 software used to measure size, where a particle's diameter was determined as the mean of three cross-sectional measurements. USPIO diameter had a lognormal distribution, where the geometric mean diameter was 9.2 nm (std dev = 1.1 nm). Silica layer thickness after final silica encapsulation was 3.6 nm (std dev = 0.47 nm). A one-tail t-test comparing final particle silica layer thickness to synthesis steps pre- and post-dye conjugation was significant at p = 3.27e-6 and p = 5.88e-7, respectively. The hydrodynamic diameter by number distribution and zeta potential of the SCION particles were evaluated using

a Malvern Zetasizer Nano ZS dynamic light scattering instrument. Adjustments in pH were made with potassium hydroxide and hydrochloric acid. Hydrodynamic diameter and zeta potential relate when examining flocculation and colloidal stability. When the zeta potential is low (-30mV < ζ < 30mV), electrostatic repulsion is not strong enough to prevent the particles from aggregating. SCION point of zero charge (PZC) was found to be at pH 2.5. In the pH range where the zeta potential was low, the hydrodynamic diameter was higher, with its peak near the PZC. In the range above pH 5, a strong negative zeta potential allowed the particles to remain in suspension with a diameter of ~18 nm. This hydrodynamic diameter was similar to the TEM measurements of ~16-17 nm. SCION's stable negative charge in the pH range of 6-7 is desirable for biomedical application because it imitates the negative charge of most biomolecules [20].

SCION iron content was analyzed in duplicate by inductively coupled plasma optical emission spectrometry (Colombia Analytical Services, Tucson, Arizona) and yielded 4.46 mmol Fe/g SCION.

To characterize the particle's magnetic behavior, magnetic hysteresis and blocking temperature were analyzed with a superconducting quantum interference device (Quantum Design MPMS XL). The SCION particles demonstrated superparamagnetic behavior with tight hysteresis curves and no losses. The blocking temperature where material begins to demonstrate superparamagnetism dropped from 162.4K for uncoated USPIOs to 82.2K for silica-coated USPIOs. The results indicated that silica effectively suppresses magnetic dipolar interaction between particles, as the blocking temperature of single particles is always lower than that of agglomerated nanocrystals. Uncoated particles may agglomerate because their large surface-area-to-volume ratio enables strong magnetic dipolar interaction.

Thus, the fluorescence of SCION with 635 nm excitation was checked using Perkin Elmer LS55 fluorescence spectrophotometer. As is demonstrated in Figure 2, the particle had clear strong emissions when compared to the control of unlabeled USPIOs.

Particle Diameter	**TEM**	~16-17 nm
	DLS	~18 nm
Point of Zero Charge		pH 2.5
Iron Content		16400 (mol Fe)(mol SCION)$^{-1}$
		~4.46 (mmol Fe)(g SCION)$^{-1}$
Superparamagnetism		No magnetic hysteresis losses
Blocking Temperature		82.2 K

Table 1: SCION properties.

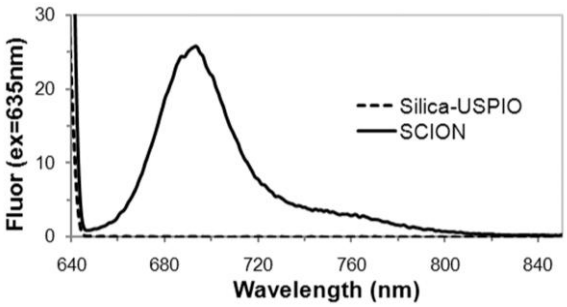

Figure 2: Fluorescence spectrum of SCION and unlabeled USPIO with excitation at 635nm.

4 *IN VIVO* IMAGING APPLICATIONS

A number of different applications of these particles are being studied in mice models, both tumor bearing and non-tumor bearing. Examples are presented below in Figures 3 and 4, where the first is demonstration of the tri-imageability of the in a subcutaneous tumor model and the second a dual MR/optical application of particle for sentinel lymph node imaging. Initial *in vivo* studies of untargeted SCION reveal quick blood clearance and high uptake in the liver and spleen.

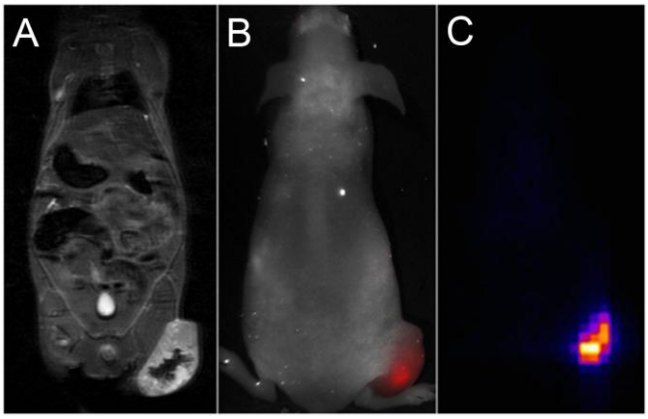

Figure 3: Tri-imageable SCION intratumoral injection into subcutaneous LS-174T colon carcinoma mouse model. (A) MR T2-weighted images 2 hr post-injection. (B) Optical image (composite of spectrally unmixed white light and NIR light) at 2 hr post-SCION injection. (C) γ-scintigraphy image at 4 hr post-SCION injection.

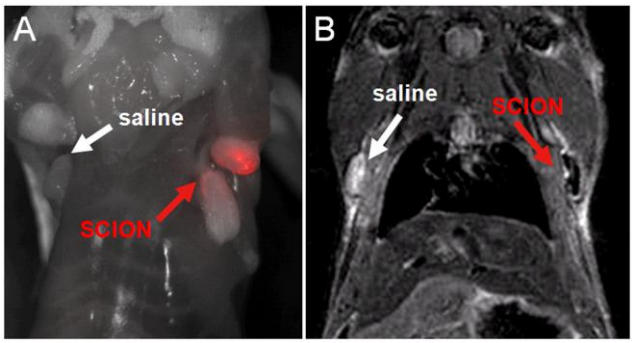

Figure 4: Sentinel lymph node detection by (A) optical and (B) T2-weighted MR images after intradermal injections of SCION or control saline solution in front footpad.

5 DISSCUSSION

During each phase of development, SCION has been characterized for surface charge, structure by transmission electron microscopy and dynamic light scattering, and optical response by fluorescence spectrophotometry. Magnetic properties including hysteresis measurements and field cooling analyses were conducted using a superconducting quantum interference device.

Although the size is an advantage for passive delivery, to actively direct SCIONs to a specific location (i.e. epithelial cancers or multiple sclerosis inflammatory foci), various antibodies have been attached to the particle surface. The chelator CHXA"-DTPA was conjugated to antibody and the entire nanoparticle-antibody construct successfully labeled with ^{111}In. Biodistribution, pharmacokinetics, MR, optical, and nuclear imaging studies were conducted and the results demonstrate SCION's potential for application *in vivo*, particularly much promise in the area of sentinel node imaging. Accurate characterization of the first draining lymph node in primary tumors is a challenging task where current methods rely on nodal size as the primary yardstick for differentiating benign from malignant nodes. Other parameters such as the nodal shape, contour, and level of enhancement may also provide useful information. Currently, two agents are used for sentinel node imaging, blue dye isosulfan and a radiolabeled macromolecule, i.e. 99mTc-albumin or sulfur colloid. *In vivo* optical and MR imaging of athymic mice given intracutaneous injection of SCION in the foot pad reveal visualization of the primary draining lymph nodes. Unlike previous techniques, the particle could first be used to characterize lymph nodes by MR, followed by fluorescence identification during surgery, and further histology using its fluorescence and iron content.

As currently synthesized, the nanoparticles can be used for diagnostics; however, they can also be developed into a method of thermotherapy. Once the delivery construct is traced to its target location, its superparamagnetic properties can be exploited by the application of an AC magnetic field to heat tissue or activate a drug. Thus, with conjugates of this nanoparticle, it should be possible to target specific tissues, verify localization and then non-invasively activate multimodal therapies using extrinsic fields.

REFERENCES

[1] Andersson-Engels S and Wilson B C 1992 *J. Cell Pharmacol.* **3** 48
[2] Bumb A, Brechbiel M W, Choyke P L, et al 2008 *Nanotechnology* **19** 335601
[3] Bumb A, Regino C A S, Perkins M R, et al 2010 *Nanotechnology* **21** 175704
[4] Coroiu I 1999 *Journal of Magnetism and Magnetic Materials* **201** 449
[5] Grosenick D, Wabnitz H, Rinneberg H, et al 1999 *App. Opt.* **38** 2927
[6] Huang S, Armstrong E A, Benavente S, et al 2004 *Cancer Res* **64** 5355
[7] Huneke R B, Pippin C G, Squire R A, et al 1992 *Cancer Research* **52** 5818
[8] Jin Y, Kannan S, Wu M, et al 2007 *Chem. Res. Toxicol.* **20** 1126
[9] Krogsgaard M, Wucherpfennig K W, Cannella B, et al 2000 *The Journal of experimental medicine* **191** 1395
[10] Liu D M and Chen I W 1999 *Acta Materialia* **47** 4535
[11] Madsen L S, Andersson E C, Jansson L, et al 1999 *Nat Genet* **23** 343
[12] McDevitt M R, Barendswaard E, Ma D, et al 2000 *Cancer Research* **60** 6095
[13] Milenic D E, Garmestani K, Brady E D, et al 2004 *Clinical cancer research* **10** 7834
[14] Milenic D E, Garmestani K, Chappell L L, et al 2002 *Nuclear Medicine and Biology* **29** 431
[15] Mujumdar S R, Mujumdar R B, Grant C M, et al 1996 *Bioconj. Chem.* **7** 356
[16] Mulvaney P, Liz-Marzan L M, Giersig M, et al 2000 *J.Mater.Chem.* **10** 1259
[17] Santra S, Zhang P, Wang K M, et al 2001 *Analytical Chemistry* **73** 4988
[18] Swadeshmukul S, Kemin W, Rovelyn T, et al 2001 *J Biomedical Optics* **6** 160
[19] Ulman A 1996 *Chem.Rev.* **96** 1533
[20] Vroman L 1974 *Science* **184** 585
[21] Wagnières G A, Star W M and Wilson B C 1998 *Photochem. Photobiol.* **68** 603
[22] Weissleder R 2001 *Nat. Biotech.* **19** 316
[23] Xu H, Baidoo K, Gunn A J B, C.A., et al 2007 *J. Med. Chem.* **50** 4759
[24] Xue Z, Liang D, Li Y, et al 2005 *Chin. Sci. Bull.* **20** 2323